Globally Exponentially Stable Aided Inertial Navigation with Hydroacoustic Measurements from A Single Transponder

Bård B. Stovner[1], Tor A. Johansen[2], Ingrid Schjølberg[1]

***Abstract*— This paper provides a novel formulation relating underwater range measurements to body-fixed position when several acoustic transceivers are mounted on the vehicle and only one transponder is placed in the vehicle's surroundings. This formulation is used in a novel three-stage filter for aided inertial navigation that has both global convergence and near-optimal performance w.r.t. variance of the estimate. It estimates both the position and velocity of the vehicle, and relies on a globally stable attitude observer to provide estimates of the attitude and angular rate sensor bias. Two different formulations of the novel three-stage filter were tested in simulations and shown to track the true position.**

I. Introduction

Underwater navigation in missions covering large underwater areas is challenging and an important field of research. Installing and maintaining fixed infrastructure that facilitate positioning is expensive, and should be minimized for cost reduction. An example of such missions is an underwater intervention vehicle in transit between subsea oil and gas installations. In this paper, the problem of position and velocity estimation of a vehicle with only one available sea floor mounted transponder is considered. It is well known that with three or more transponders, the position can be estimated in the inertial frame. Examples of such systems are long baseline (LBL) and short baseline (SBL) where three or more transponders are mounted on the sea floor or the underside of a surface vessel, respectively. In applications where a surface vessel is available, the ultra-short baseline (USBL) can also be used, in which a compact array of transducers are mounted to the underside of the surface vessel. When only one transponder is available, however, the vehicle either needs to collect range measurements over time, as was studied by Batista, Silvestre, and Oliveira [1], or have multiple transceivers mounted to it, as was done by Batista, Silvestre, and Oliveira [2], in order for the position estimation problem to be observable. An example of the latter is the inverted USBL (iUSBL) system, where an USBL transceiver is mounted on the underwater vehicle, capable of providing range and relative attitude measurements between the vehicle and the transponder. In this paper, a set up is suggested in which multiple transceivers are mounted as far as possible from each other on an underwater vehicle. This set up is named *inverted SBL* (iSBL) since it shares the property with SBL that the baseline lengths are confined by the size of the vehicle to which it is mounted. This is contrary to iUSBL, where the baseline lengths are confined to the size of the iUSBL apparatus in which the transducers lie. Where the short baselines of iUSBL necessitate highly accurate phase difference measurements, the longer baselines of the iSBL has the potential of relaxing this accuracy requirement. Furthermore, instead of measuring the range and relative attitude between transponder and vehicle, the iSBL uses the individual ranges to, or range differences between, the vehicle mounted hydrophones. This facilitates tightly coupled integration of inertial and hydroacoustic measurements. A similar set up was studied in Batista, Silvestre, and Oliveira [2], except the baselines between the hydrophones were short as in iUSBL, but the range differences between hydrophones were used as measurements, requiring highly accurate phase measurements. The suggested set up is coined iSBL in order to avoid confusion with iUSBL technology.

The overall goal of the presented work is the development of a novel three-stage filter for aided inertial navigation using an iSBL system. It builds on the work of Johansen and Fossen [3], [4], where a non-linear model is linearized about a suboptimal and globally stable estimate, and a Kalman filter (KF) is implemented based on the linearized model. The estimate from the linearized KF is shown to inherit the stabilty properties of the suboptimal estimate while yielding better performance w.r.t. variance. In Johansen, Fossen, and Goodwin [5], a three-stage filter for position estimation of a unmanned aerial vehicle provided earth-fixed radio beacons was developed. A three-stage filter for an underwater vehicle provided an LBL system was presented in Stovner et al. [6]. In both works, the position and velocity were estimated in the North-East-Down (NED) frame. Morgado et al. [7] developed a globally asymptotically stable (GAS) filter fusing iUSBL and measurements from an inertial measurement unit (IMU). Since the iUSBL measurement can be used straightforwardly to find the position of the transponder relative the vehicle in the body-fixed frame, the position estimation is conducted in this frame as well. Unlike the iUSBL, the iSBL measures separate ranges to all transceivers. Therefore, the iSBL set up facilitates implementation of estimation of the translational motion both in the NED and the body-fixed frames. In the presented work, filters using both of these formulations are developed and compared. Since both formulations require an attitude estimate, a globally exponentially stable (GES) non-linear attitude observer (NLAO) is implemented.

[1] Department of Marine Technology, University of Science and Technology (NTNU), 7491 Trondheim, Norway.
[2] Department of Engineering Cybernetics, NTNU, 7491 Trondheim, Norway.

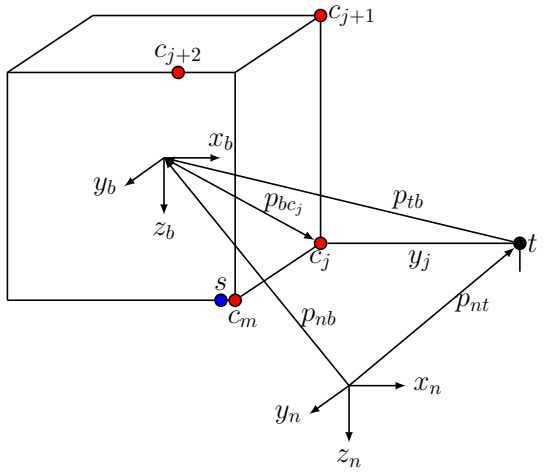

Fig. 1. The configuration of iSBL hydrophones (red), transmitter (blue), and the transponder (black).

A. Scope and Outline

The main contribution of this paper is a globally exponentially stable three-stage filter for position and velocity estimation using iSBL and IMU measurements. Two different formulations of the novel three-stage filter are tested and verified in simulations. The use of such a filter for position and velocity estimation is highly relevant for underwater applications where installing fixed infrastructure is expensive and demanding. The estimation error dynamics is shown to be GES for weakly accelerated vehicles, which makes the estimation strategy rather insensitive to initialization errors.

II. Models and Preliminaries

A. Notation

The position, velocity, and angular rate of a vehicle are denoted p^a_{bc}, v^a_{bc}, and ω^a_{bc}, respectively, where p^a_{bc} denotes the position of c relative b decomposed in the coordinate frame $\{a\}$. A rotation matrix expressing the rotation from the frame $\{b\}$ to $\{a\}$ is denoted R^a_b.

In this notation, we define the body-fixed translational state vector

$$x \triangleq \begin{bmatrix} p^b_{tb} \\ v^b_{nb} \end{bmatrix} \tag{1}$$

where p^b_{tb} is the position of the vehicle relative to the transponder t decomposed in the body-fixed frame $\{b\}$. Furthermore, v^b_{nb} is the velocity of the vehicle relative the North-East-Down (NED) frame $\{n\}$ decomposed in the body-fixed frame.

We also define the inertial translational state vector

$$\chi \triangleq \begin{bmatrix} p^n_{nb} \\ v^n_{nb} \end{bmatrix} \tag{2}$$

Lastly, we denote by z the vector of variables (R^n_b, b^b_{ars}) where R^n_b is the rotation matrix from NED to the body-fixed frame $\{b\}$, and b^b_{ars} is the angular rate sensor (ARS) bias.

B. Model

1) Measurements: Let there be M transceivers on the vehicle. Let $p^b_{bc_j}$ be the position of transceiver c_j relative the origin of the body-fixed frame. Assume a transmitting transducer is mounted next to transceiver c_m, which is responsible for contacting the transponder. Further assume that the vehicle moves slowly relative to the speed of sound. Now, when hydrophone c_m detects the time-of-arrival (TOA), it measures the travel from transmitter to transponder and back in addition to noise: $2\|p^b_{tb} + p^b_{bc_m}\|_2 + \epsilon_y + \epsilon_{\partial,m}$. Therefore, we model the range measurement y_m by

$$y_m = h_m(x) \triangleq \|p^b_{tb} + p^b_{bc_m}\|_2 + \frac{1}{2}\epsilon_y + \frac{1}{2}\epsilon_{\partial,m} \tag{3}$$

where it is assumed that $\epsilon_y \sim \mathcal{N}(0, \sigma_y^2)$ is a noise term common for all hydrophones, and $\epsilon_{\partial,j} \sim \mathcal{N}(0, \sigma_\partial^2), j = (1, ..., M)$ is a noise term unique for hydrophone c_j. The TOA at hydrophone $c_j = (1, ..., M)\backslash m$ measures the distance plus noise $\|p^b_{tb}+p^b_{bc_m}\|_2+\|p^b_{tb}+p^b_{bc_j}\|_2+\epsilon_y+\epsilon_{\partial,j}$, from which the range measurement y_j can be found by subtracting y_m:

$$y_j = h_j(x) \triangleq \|p^b_{tb} + p^b_{bc_j}\|_2 + \frac{1}{2}\epsilon_y + \epsilon_{\partial,j} - \frac{1}{2}\epsilon_{\partial,m} \tag{4}$$

Since σ_y is typically much larger than σ_∂, we find the range difference measurements in which ϵ_y vanish

$$\begin{aligned} \partial y_j =& \partial h_j(x) \triangleq h_j(x) - h_m(x) \\ =& \|p^b_{tb} + p^b_{bc_j}\|_2 - \|p^b_{tb} + p^b_{bc_m}\|_2 + \epsilon_{\partial,j} - \epsilon_{\partial,m} \end{aligned} \tag{5}$$

Now, we define the vectors of range and range difference measurement vectors

$$\begin{aligned} y &= \begin{bmatrix} y_1 & \cdots & y_m & \cdots & y_M \end{bmatrix}^\top \\ h(x) &= \begin{bmatrix} h_1(x) & \cdots & h_m(x) & \cdots & h_M(x) \end{bmatrix}^\top \\ \partial y &= \begin{bmatrix} \partial y_1 & \cdots & y_m \cdots & \partial y_M \end{bmatrix}^\top \\ \partial h(x) &= \begin{bmatrix} \partial h_1(x) & \cdots & h_m(x) & \cdots & \partial h_M(x) \end{bmatrix}^\top \end{aligned}$$

Note that the measurement models also can be expressed in the NED frame through the equality

$$\|p^b_{tb} + p^b_{bc_j}\|_2 \equiv \|p^n_{nb} - p^n_{nt} + R^n_b p^b_{bc_j}\|_2 \tag{6}$$

and thus, $h(x) \equiv h(\chi, z)$ and $\partial h(x) \equiv \partial h(\chi, z)$.

The angular rate ω^b_{nb} and acceleration a^b_{nb} are observed through the ARS and accelerometer measurements modelled as

$$\omega^b_{ars} = \omega^b_{nb} + b^b_{ars} + \epsilon_{ars} \tag{7}$$

$$f^b_{acc} = a^b_{nb} - R^\top(q^n_b)g^n + \epsilon_{acc} \tag{8}$$

respectively. ϵ_{ars} and ϵ_{acc} are assumed to be unbiased, Gaussian noises with $\epsilon_{ars} \sim \mathcal{N}(0, \sigma^2_{ars})$ and $\epsilon_{acc} \sim \mathcal{N}(0, \sigma^2_{acc})$.

The normalized magnetometer measurement vector m^b is modelled as

$$m^b = R^{n\top}_b m^n + \epsilon_{mag}$$

where m^n is a known NED reference vector at the location and the magnetometer noise is assumed given by $\epsilon_{mag} \sim \mathcal{N}(0, \sigma^2_{mag})$.

2) Dynamics: The dynamics of R_b^n and b_{ars}^b are

$$\dot{R}_b^n = R_b^n S(\omega_{nb}^b) \tag{9a}$$
$$\dot{b}_{ars}^b = 0 \tag{9b}$$

where $S(\cdot)$ is the skew-symmetric matrix

$$S(\omega) = \begin{bmatrix} 0 & -\omega_3 & \omega_2 \\ \omega_3 & 0 & -\omega_1 \\ -\omega_2 & \omega_1 & 0 \end{bmatrix}$$

The dynamics of the body-fixed translational motion state is

$$\dot{p}_{tb}^b = -S(\omega_{ars}^b - b_{ars}^b)p_{tb}^b + v_{nb}^b \tag{10a}$$
$$\dot{v}_{nb}^b = -S(\omega_{ars}^b - b_{ars}^b)v_{nb}^b + a_{nb}^b \tag{10b}$$

Inserting (7)–(8) into (10) and writing it in matrix form yields

$$\dot{x} = A_x(t,z)x + B_x(z)u + G_x(x)\epsilon_x \tag{11}$$

where

$$A_x(t,z) = \begin{bmatrix} -S(\omega_{ars}^b - b_{ars}^b) & I \\ 0 & -S(\omega_{ars}^b - b_{ars}^b) \end{bmatrix}$$
$$B_x(z) = \begin{bmatrix} 0 & 0 \\ I & R_b^{n\top} \end{bmatrix},\ u(t) = \begin{bmatrix} f_{acc}^b \\ g^n \end{bmatrix}$$
$$G_x(x) = \begin{bmatrix} -S(p_{tb}^b) & 0 \\ -S(v_{nb}^b) & -I \end{bmatrix}, \epsilon_x = \begin{bmatrix} \epsilon_{ars} \\ \epsilon_{acc} \end{bmatrix}$$

The dynamics of the inertial translational motion state is

$$\dot{p}_{nb}^n = v_{nb}^n \tag{12a}$$
$$\dot{v}_{nb}^n = R_b^n(-b_{ars}^b + f_{acc}^b) + g^n \tag{12b}$$

Inserting (8) into (12) yields

$$\dot{\chi} = A_\chi \chi + B_\chi(z)u + G_\chi \epsilon_\chi \tag{13}$$

$$A_\chi = \begin{bmatrix} 0 & I \\ 0 & 0 \end{bmatrix}, B_\chi(z) = \begin{bmatrix} 0 & 0 \\ R_b^n & I \end{bmatrix}$$
$$G_\chi(z) = \begin{bmatrix} 0 \\ R_b^n \end{bmatrix}, \epsilon_\chi = \epsilon_{acc}$$

III. Three-stage Filter Development

The filter to be developed consist of three stages. In the first stage, an algebraic non-linear transformation (ANT) gives a new, globally valid, and linear measurement model from the non-linear one. In the second stage, a linear time-varying (LTV) Kalman filter (KF) is implemented, based on the linear measurements model found by the ANT and the linear dynamics. GES of the LTV KF follows from the uniform complete observability (UCO) of the LTV model. However, the ANT neglects the effect of measurement noise, and consequently, the estimate from stage 2 is far from optimal w.r.t. variance. This performance loss is recovered in stage 3, where a KF based on a linearization of the non-linear measurement model about the estimate from the second stage is implemented. This cascade of stages, seen in Figure 2, preserves the stability properties while giving near-optimal estimation performance w.r.t. variance [3].

Estimates and variables associated with stage 1, 2, and 3 are marked with $\underline{(\cdot)}$, $\bar{(\cdot)}$, and $\hat{(\cdot)}$, respectively.

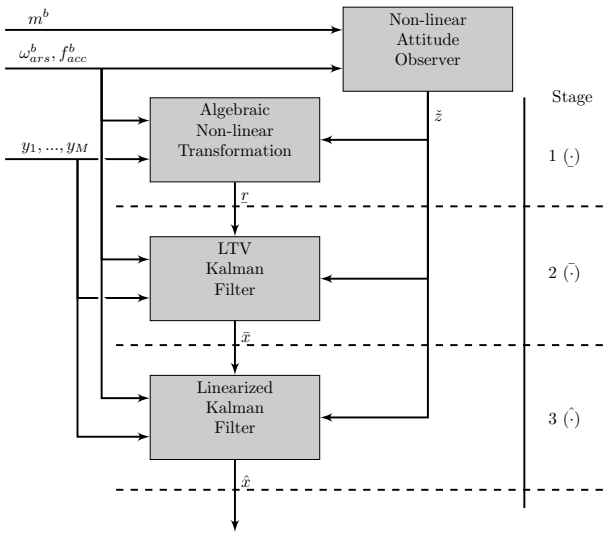

Fig. 2. In this figure, the three stages of the body-fixed three-stage filter are depicted. The stage number and the associated notation can be seen on the right-hand side.

A. Non-linear Attitude Observer

For attitude estimation, we use in this paper the NLAO from [8]. The estimate $\check{z}$ is found by

$$\dot{\check{R}}_{\check{b}}^n = \check{R}_{\check{b}}^n S(\omega_{ars}^b - \check{b}^{\check{b}}) + \sigma K_p J \tag{14a}$$
$$\dot{\check{b}}^{\check{b}} = -\text{Proj}(\check{b}^{\check{b}}, -k_I \text{vex}(\mathbb{P}(\check{R}_{\check{b}}^{n\prime} K_p J))) \tag{14b}$$

where

$$J = \sum_{k=1}^{3} (\nu_k^n - \hat{R}_{\hat{b}}^n \nu_k^b)\nu_k^{b\top}$$

$$\nu_1^n = \frac{g^n}{\|g^n\|} \quad \nu_2^n = \frac{S(g^n)m^n}{\|S(g^n)m^n\|} \quad \nu_3^n = \frac{S^2(g^n)m^n}{\|S^2(g^n)m^n\|}$$
$$\nu_1^b = \frac{f_{acc}^b}{\|f_{acc}^b\|} \quad \nu_2^b = \frac{S(f_{acc}^b)m^b}{\|S(f_{acc}^b)m^b\|} \quad \nu_3^b = \frac{S^2(f_{acc}^b)m^b}{\|S^2(f_{acc}^b)m^b\|}$$

and k_I, K_p, and σ are tuning parameters. The function $\mathbb{P}(X) = \frac{1}{2}(X - X^\top)$ for square matrices X, and $\text{vex}(S(x)) = x$ for $x \in \mathbb{R}^3$. $\text{Proj}(\check{b}_{ars}^{\check{b}}, \beta)$ is a projection function designed to keep the estimate $\check{b}_{ars}^b$ within a ball of radius M_b in which we assume the true ARS bias b_{ars}^b to lie [8]. Notice that the use of g^n assumes a weakly accelerated vehicle, i.e. $f_{acc}^b \approx R^\top(q_b^n)g^n$.

B. Stage 1

Stage 1 consists of an algebraic non-linear transformation. In the further derivations in this section, noise is neglected. First, the body-fixed formulation is treated before the formulation in NED.

1) Body-fixed formulation: By algebraic manipulation of (4), Y_x is constructed:

$$y_j^2 = \|p_{tb}^b\|^2 + 2{p_{bc_j}^b}^\top p_{tb}^b + \|p_{bc_j}^b\|^2, j \in (1, ..., M) \tag{15}$$
$$\Rightarrow Y_x - l r_x = C_{xp} p_{tb}^b \tag{16}$$

where

$$Y_x = \begin{bmatrix} y_1^2 - \|p_{bc_1}^b\|^2 \\ \vdots \\ y_M^2 - \|p_{bc_M}^b\|^2 \end{bmatrix}, C_{xp} = \begin{bmatrix} 2p_{bc_1}^{b\top} \\ \vdots \\ 2p_{bc_M}^{b\top} \end{bmatrix}, l = \begin{bmatrix} 1 \\ \vdots \\ 1 \end{bmatrix} \tag{17}$$

and $r_x = \|p_{tb}^b\|^2$. Assuming $M \geq 3$ and $\text{rank}(C_{xp}) = 3$, we can find $c_x = C_{xp}^\dagger l$ and $w_x = C_{xp}^\dagger Y_x$, where † denotes the Moore-Penrose pseudo-inverse, which gives us

$$p_{tb}^b = -r_x c_x + w_x \tag{18}$$

Inserting this into $r_x = \|p_{tb}^b\|_2^2$ yields

$$r_x^2 \|c_x\|_2^2 - r_x \underbrace{(2c_x^\top w_x + 1)}_{h_x} + \|w_x\|_2^2 = 0$$

which has two solutions $\underline{r}_x$ and $\underline{\underline{r}}_x$

$$\underline{r}_x, \underline{\underline{r}}_x = \frac{h_x \pm \sqrt{h_x^2 - 4\|c_x\|_2^2 \|w_x\|_2^2}}{2\|c_x\|_2^2} \tag{19}$$

when $\|c_x\| \neq 0$ and the solution $\underline{r}_x = \frac{\|w_x\|_2^2}{h_x}$ when $\|c_x\| = 0$. Assuming this ambiguity can be resolved when $\|c_x\| \neq 0$, and the correct solution, which we denote $\underline{r}_x$, can be selected, we have successfully constructed a linear measurement equation

$$Y_x + l\underline{r}_x = C_{xp} p_{tb}^b = C_x x \tag{20}$$

where $C_x = \begin{bmatrix} C_{xp} & 0 \end{bmatrix}$.

Remark 1: If we insert the two solutions $\underline{r}_x$ and $\underline{\underline{r}}_x$ into (18), we will get two estimates $\underline{p}_{tb}^b$ and $\underline{\underline{p}}_{tb}^b$ of p_{tb}^b, respectively. In selecting the correct solution $\underline{r}_x$, one can be helped by e.g. comparing the z-values of $R(q_b^n)\underline{p}_{tb}^b$ and $R(q_b^n)\underline{\underline{p}}_{tb}^b$ with depth measurements.

2) NED formulation: The derivation of the ANT for the NED formulation will be similar to that in Section III-B.1, but starting with the measurement model (4) expressed by the right hand side of (6):

$$y_j^2 = \|R_b^n p_{bc_j}^b - p_{nt}^n\|_2^2 + 2(R_b^n p_{bc_j}^b - p_{nt}^n)^\top p_{nb}^n + r_\chi$$

where $r_\chi = \|p_{nb}^n\|_2^2$. Now we form

$$Y_\chi = \begin{bmatrix} y_1^2 - \|R_b^n p_{bc_j}^b - p_{nt}^n\|_2^2 \\ \vdots \\ y_M^2 - \|R_b^n p_{bc_M}^b - p_{nt}^n\|_2^2 \end{bmatrix}$$

$$C_{\chi_p}(z) = \begin{bmatrix} 2(R_b^n p_{bc_1}^b - p_{nt}^n)^\top \\ \vdots \\ 2(R_b^n p_{bc_M}^b - p_{nt}^n)^\top \end{bmatrix}$$

and we get the linear measurement model

$$Y_\chi - l\underline{r}_\chi = C_\chi(z) p_{nb}^n \tag{21}$$

where $C_\chi(z) = \begin{bmatrix} C_{\chi_p}(z) & 0 \end{bmatrix}$ and $\underline{r}_\chi$ is found in the same way as $\underline{r}_x$.

C. Stage 2

In stage 2, an LTV KF is implemented based on the linear measurement equation from the ANT in stage 1. First, the body-fixed LTV KF is developed, and then the NED LTV KF.

1) LTV KF with body-fixed formulation:

$$\dot{\bar{x}} \triangleq A_x(t, \check{z})\bar{x} + B_x(\check{z})u(t) + \bar{K}_x(t)(Y_x + l\underline{r}_x - C_x\bar{x}) \tag{22}$$

where $\bar{K}_x(t)$ is the standard time-varying KF gain matrix.

The process noise covariance matrix is

$$Q_x = \text{E}(\epsilon_x \epsilon_x^\top) = \text{diag}(\sigma_{ars}^2 l_3, \sigma_{acc}^2 l_3) \tag{23}$$

where $l_3 \in \mathbb{R}^3$ is a vector of ones, and the G-matrix is $G_x(\bar{x})$.

The measurement noise covariance matrix is

$$\bar{R} = \text{Cov}(Y, Y) = \text{E}\left[(Y - \text{E}(Y))(Y - \text{E}(Y))^\top\right] \tag{24}$$

whose elements are given by

$$\begin{aligned}
\text{Cov}(Y_j, Y_j) &= y_j^2(\sigma_y^2 + \sigma_\partial^2) + \frac{1}{8}\sigma_y^4 + \frac{5}{4}\sigma_y^2\sigma_\partial^2 + \frac{25}{8}\sigma_\partial^4 \\
\text{Cov}(Y_j, Y_i) &= y_i y_j(\sigma_y^2 + 5\sigma_\partial^2) + \frac{1}{8}\sigma_y^4 + \frac{1}{4}\sigma_y^2\sigma_\partial^2 + \frac{9}{8}\sigma_\partial^4 \\
\text{Cov}(Y_j, Y_m) &= y_j y_m(\sigma_y^2 - \sigma_\partial^2) + \frac{1}{8}\sigma_y^4 + \frac{1}{8}\sigma_\partial^4 \\
\text{Cov}(Y_m, Y_m) &= y_m^2(\sigma_y^2 + \sigma_\partial^2) + \frac{3}{16}\sigma_y^4 + \frac{3}{8}\sigma_y^2\sigma_\partial^2 + \frac{3}{16}\sigma_\partial^4
\end{aligned}$$

2) LTV KF with NED formulation:

$$\dot{\bar{\chi}} \triangleq A_\chi \bar{\chi} + B_\chi(\check{z})u + \bar{K}_\chi(Y_\chi + l\underline{r}_\chi - C_\chi(\check{z})\bar{\chi}) \tag{25}$$

where $\bar{K}_\chi(t)$ is the standard time-varying KF gain matrix. The process covariance matrix is

$$Q_\chi = E(\epsilon_\chi \epsilon_\chi^\top) = I_3 \sigma_{acc}^2 \tag{26}$$

and the G-matrix is $G_\chi(\check{z})$. The measurement noise covariance matrix is $\bar{R}$.

An implicit assumption that has been made here, is that $\underline{r}_x$ and $\underline{r}_\chi$ is noise-free, which is not true. Modelling the noise from the r-term is difficult and not regarded here, but would yield better performance. The work of Jørgensen, Johansen and Schjølberg [9] improved on the three-stage filter of Stovner et al. [6] by modelling the noise in the r-term by a numerical method. A similar strategy could have been used here, which is assumed to improve the performance of the LTV KFs.

D. Stage 3

The third stage consists of a KF based on the linearization of the non-linear measurement model about the estimate from stage 2. As before, we derive the linearized KF with the body-fixed formulation before the linearized KF with the NED formulation.

1) Linearized KF with body-fixed formulation: The linearization is found by the Taylor expansion

$$\partial h_j(x) = \partial h_j(\bar{x}) + H_{xp,j}(\bar{x})(x - \bar{x}) + \varphi_j(x, \bar{x}) \quad (27)$$

where $\varphi_j(x, \bar{x})$ represents higher order terms. We write the vector $H_{x,j}(\bar{x}) = \begin{bmatrix} H_{xp,j} & 0 \end{bmatrix}$ and find

$$H_{xp,j}(\bar{x}) = \left.\frac{\mathrm{d}\partial h_j(x)}{\mathrm{d}p^b_{tb}}\right|_{x=\bar{x}} = \frac{(\bar{p}^{\check{b}}_{tb} + p^b_{bc_j})^\top}{\|\bar{p}^{\check{b}}_{tb} + p^b_{bc_j}\|_2} - \frac{(\bar{p}^{\check{b}}_{tb} + p^b_{bc_m})^\top}{\|\bar{p}^{\check{b}}_{tb} + p^b_{bc_m}\|_2}$$

Concatenating for $j \in (1, ..., M)$ gives us the linearized measurement matrix $H(\bar{x})$

$$H_{xp}(\bar{x}) = \begin{bmatrix} H_{p1}(\bar{x}) \\ \vdots \\ H_{pM}(\bar{x}) \end{bmatrix}, H_x(\bar{x}) = \begin{bmatrix} H_{xp}(\bar{x}) & 0 \end{bmatrix}$$

Now, we define the estimator

$$\dot{\hat{x}} = A_x(t, \check{z})\hat{x} + B_x(\check{z})u(t) \quad (28)$$
$$+ \hat{K}_x(t)(\partial y - \partial h(\bar{x}) - H_x(\bar{x})(\hat{x} - \bar{x})) \quad (29)$$

where $\hat{K}_x$ is the standard time-varying KF gain matrix, and the G-matrix $G_x(\hat{x})$. The covariance matrix Q_x is the same as in (23) while the elements of $\hat{R}$ are given by

$$\begin{aligned} \mathrm{Cov}(\partial y_j, \partial y_i) &= \mathrm{E}[(\epsilon_{\partial,j} - \epsilon_{\partial,m})(\epsilon_{\partial,i} - \epsilon_{\partial,m})] \\ &= \mathrm{E}(\epsilon_{y,j}\epsilon_{y,i}) + \mathrm{E}(\epsilon_{y,m}\epsilon_{y,m}) \\ &= \begin{cases} 2\sigma^2_\partial, i = j \\ \sigma^2_\partial, i \neq j \end{cases} \end{aligned} \quad (30a)$$

$$\begin{aligned} \mathrm{Cov}(\partial y_j, y_m) &= \mathrm{E}[(\frac{1}{2}\epsilon_y + \frac{1}{2}\epsilon_{\partial,m})(\epsilon_{\partial,i} - \epsilon_{\partial,m})] \\ &= -\frac{1}{2}\sigma^2_\partial \end{aligned} \quad (30b)$$

$$\mathrm{Cov}(y_m, y_m) = \mathrm{E}[(\frac{1}{2}\epsilon_y + \frac{1}{2}\epsilon_{\partial,m})^2] = \frac{1}{4}(\sigma^2_y + \sigma^2_\partial) \quad (30c)$$

2) Linearized KF with NED formulation: We perform the Taylor expansion of (4) expressed by the right-hand side of (6) about the estimate from stage 2

$$\partial h_j(\chi, \check{z}) = \partial h_j(\bar{\chi}, \check{z}) + H_{\chi,j}(\bar{\chi})(\chi - \bar{\chi}) + \varphi_j(\chi, \bar{\chi}, \check{z}) \quad (31)$$

where $\varphi_j(\chi, \bar{\chi}, \check{z})$ represents higher order terms and

$$H_{\chi,j}(\bar{\chi}, \check{z}) = \left.\frac{\mathrm{d}\partial h_{\chi,j}(\chi, \check{z})}{\mathrm{d}p^n_{nb}}\right|_{\chi=\bar{\chi}}$$
$$= \frac{(\bar{p}^n_{nb} + R^n_{\check{b}}p^b_{bc_j} - p^n_{nt})^\top}{\|\bar{p}^n_{nb} + R^n_{\check{b}}p^b_{bc_j} - p^n_{nt}\|_2} - \frac{(\bar{p}^n_{nb} + R^n_{\check{b}}p^b_{bc_m} - p^n_{nt})^\top}{\|\bar{p}^n_{nb} + R^n_{\check{b}}p^b_{bc_m} - p^n_{nt}\|_2}$$

Stacking this yields

$$H_{\chi_p}(\bar{\chi}, \check{z}) = \begin{bmatrix} H_{\chi,1}(\bar{\chi}, \check{z}) \\ \vdots \\ H_{\chi,M}(\bar{\chi}, \check{z}) \end{bmatrix}, H_\chi(\bar{\chi}, \check{z}) = \begin{bmatrix} H_{\chi_p}(\bar{\chi}, \check{z}) & 0 \end{bmatrix}$$

Now, we define the estimator

$$\dot{\hat{\chi}} \triangleq A_\chi\hat{\chi} + B_\chi(\check{z})u$$
$$+ \hat{K}_\chi(t)(\partial y - \partial h_j(\bar{\chi}, \check{z}) - H_\chi(\bar{\chi}, \check{z})(\hat{\chi} - \bar{\chi})) \quad (32)$$

where $\hat{K}_\chi(t)$ is the standard time-varying KF gain matrix and the G-matrix is $G_\chi(\check{z})$. The process covariance matrix is Q_χ from (26) and the elements of the measurement covariance matrix are the same $\hat{R}$ as in (30).

IV. Stability Analysis

Assumption 1: The reference vectors g^n and m^n are non-parallel.

Proposition 1: Define the errors $\tilde{R} \triangleq R^n_b - \check{R}^n_{\check{b}}$ and $\tilde{b}_{ars} = b^b_{ars} - \check{b}^{\check{b}}_{ars}$. For any given choise of K_p and k_I, there exists a $\sigma^* > 1$ such that for all $\sigma > \sigma^*$, the origin $\tilde{R} = 0$ and $\tilde{b}_{ars} = 0$ of the dynamics of $\tilde{R}$ and $\tilde{b}_{ars}$ is GES.

Proof: For proof, it is referred to [8]. ∎

Assumption 2: There are at least 3 non-colinear transceivers on the vehicle.

We state a useful corollary

Corollary 1: Consider the block triangular matrix

$$M = \begin{bmatrix} D & 0 \\ E & F \end{bmatrix}$$

where D, E, and F are matrices of arbitrary dimensions. Now, if D and F have full rank, then M has full rank.

Proof: The proof follows directly from Theorem 4.2 of Meyer [10]. ∎

In the following, the stability of the three-stage filter is analyzed. We begin by analyzing the stability of the LTV KFs in stage 1. Then we use XKF theory from [3] to show that the cascade of filters is GES.

Proposition 2: The equilibrium points $\tilde{\tilde{x}} \triangleq x - \bar{x} = 0$ and $\tilde{\tilde{\chi}} \triangleq \chi - \bar{\chi} = 0$ of the error dynamics $\dot{\tilde{\tilde{x}}} = (A_x(t, \check{z}) - \bar{K}_x(t)C_x)\tilde{\tilde{x}}$ and $\dot{\tilde{\tilde{\chi}}} = (A_\chi - \bar{K}_\chi(t)C_\chi(\check{z}))\tilde{\tilde{\chi}}$ are GES, respectively.

Proof: Kalman and Bucy [11] proves that a linear time-varying system is UGES if the pair $(A(t), C(t))$ is uniformly completely observable (UCO) and $(A(t), G(t))$ is uniformly completely controllable (UCC), where $A(t)$, $C(t)$, and $G(t)$ are general process, measurement, and process noise matrices, respectively. Further, we use Theorem 6.O12 in Chen [12], which proves that the pairs $(A_x(t, \check{z}), C_x)$ and $(A_\chi, C_\chi(\check{z}))$ are UCO if the observability co-distribution formed by $A_x(t, \check{z})$ and C_x and A_χ and $C_\chi(\check{z})$, respectively, have full rank. Forming the top $2M$ rows of the observability co-distribution of the body-fixed and NED filters yields

$$\mathrm{d}\bar{\mathcal{O}}_x = \begin{bmatrix} C_{xp} & 0 \\ \star & C_{xp} \end{bmatrix} \quad (33)$$

$$\mathrm{d}\bar{\mathcal{O}}_\chi = \begin{bmatrix} C_{\chi_p}(\check{z}) & 0 \\ \star & C_{xp}(\check{z}) \end{bmatrix} \quad (34)$$

respectively. $\star$ denotes a matrix that does not influence the analysis, and is therefore unimportant. Under Assumption 2, we know that C_{xp} and $C_{\chi_p}(\check{z})$ have full rank. By Corollary 1, we know that when C_{xp} and $C_{\chi_p}(\check{z})$ have full rank, then $\mathrm{d}\bar{\mathcal{O}}_x$ and $\mathrm{d}\bar{\mathcal{O}}_\chi$ have full rank, and thus, the observability co-distributions have full rank. The proof for UCC of $(A_x(t, \check{z}), G_x(\bar{x}))$ and $(A_\chi, G_\chi(\check{z}))$ follows a similar procedure, and is straight-forward to show. This concludes the proof. ∎

Proposition 3: The respective KF tuning parameters Q, R, and $P(0)$ are chosen positive definite and symmetric in the two approaches. The equilibrium points $\tilde{\hat{x}} \triangleq x - \hat{x} = 0$ and $\tilde{\hat{\chi}} \triangleq \chi - \hat{\chi} = 0$ of the error dynamics

$$\dot{\tilde{\hat{x}}} = (A_x(t, \check{z}) - \hat{K}_x(t) H_x(\bar{x}))\tilde{\hat{x}} \tag{35}$$

$$\dot{\tilde{\hat{\chi}}} = (A_\chi - \hat{K}_\chi(t) H_\chi(\bar{\chi}, \check{z}))\tilde{\hat{\chi}} \tag{36}$$

respectively, are GES.

Proof: Using GES estimates $\bar{x}$ and $\bar{\chi}$ to linearize about, we know from Theorem 2.1 in [3] that the cascades of equilibrium points $\tilde{\bar{x}} = \tilde{\hat{x}} = 0$ and $\tilde{\bar{\chi}} = \tilde{\hat{\chi}} = 0$ of the error dynamics (35) and (36) are GES if the matrix pairs $(A_x(t, \check{z}), H_x(\bar{x}))$ and $(A_\chi, H_\chi(\bar{\chi}, \check{z}))$ are UCO and $(A_x(t, \check{z}), G_x(\hat{x}))$ and $(A_\chi, G_\chi(\check{z}))$ are UCC, respectively. We form the top $2M$ rows of the observability co-distributions which become

$$\mathrm{d}\hat{\mathcal{O}}_x = \begin{bmatrix} H_{xp}(\bar{x}) & 0 \\ \star & H_{xp}(\bar{x}) \end{bmatrix} \tag{37}$$

$$\mathrm{d}\hat{\mathcal{O}}_\chi = \begin{bmatrix} H_{\chi_p}(\bar{\chi}, \check{z}) & 0 \\ \star & H_{\chi_p}(\bar{\chi}, \check{z}) \end{bmatrix} \tag{38}$$

From Corollary 1, we know that the observability co-distributions $\mathrm{d}\hat{\mathcal{O}}_1$ and $\mathrm{d}\hat{\mathcal{O}}_2$ have full rank when $H_{xp}(\bar{x})$ and $H_{\chi_p}(\bar{\chi}, \check{z})$ have full rank. Furthermore, both matrices have full rank under Assumption 2. Therefore, $\mathrm{d}\hat{\mathcal{O}}_x$ and $\mathrm{d}\hat{\mathcal{O}}_\chi$ have full rank, and consequently, the observability co-distributions have full rank. Since the dynamics of the filters in stage 2 and 3 are similar, UCC of $(A_x(t, \check{z}), G_x(\hat{x}))$ and $(A_\chi, G_\chi(\check{z}))$ are straight-forward to show. This concludes the proof. ■

V. Simulations

Two different three-stage filters are implemented in the simulations. Stage 1 and 2 of the two filters are identical, using the body-fixed formulations in Section III-B.1 and III-C.1, respectively. In the third stage, one filter uses the body-fixed formulation of Section III-D.1, while the other uses the NED formulation of Section III-D.2. This means that the NED formulations of stage 1 in Section III-B.2 and stage 2 in Section III-C.2 are left out entirely. Using the NED formulations in stage 1 and 2 was avoided because they showed poor performance. This likely stems from C_{χ_p} becoming badly conditioned when far away from the transponder, in addition to the measurement noise being amplified in the ANT. The linearization point for the NED formulation linearized KF in stage 3 is now instead found by $\bar{\chi} = [(p^n_{nt} + \check{R}^n_{\bar{b}} \bar{p}^{\bar{b}}_{tb})^\top, (\check{R}^n_{\bar{b}} \bar{v}^{\bar{b}}_{nb})^\top]^\top$.

Although the KFs are stated earlier as continuous-time Kalman-Bucy filters, they are implemented as discrete-time KFs. Furthermore, they are updated at 100 Hz, the same frequency with which IMU measurements are assumed available. iSBL measurements are assumed retrieved at 1 Hz.

In the simulated scenario, the vehicle is box-shaped, 1.2 metres long, and has a breadth and height of 0.6 metres. In six corners of the vehicle, a transceiver is placed, i.e. $M = 6$ and

$$[p^b_{bc_1}, ..., p^b_{bc_M}] = \begin{bmatrix} 0.6 & 0.6 & 0.6 & -0.6 & -0.6 & -0.6 \\ 0.3 & 0.3 & -0.3 & 0.3 & -0.3 & -0.3 \\ 0.3 & -0.3 & 0.3 & 0.3 & -0.3 & 0.3 \end{bmatrix}$$

In practice, one can only assume that the transceivers with line-of-sight to the transponder will measure the range. Here, we assume that the six hydrophones always receive the signal. Furthermore, the sixth hydrophone has the transmitter attached to it, i.e. $m = M$. The transponder is placed at $p^n_{nt} = [-500, -500, 0]^\top$.

The initial conditions are

$$p^n_{nb}(0) = \begin{bmatrix} 0 \\ 0 \\ 0 \end{bmatrix}, v^n_{nb}(0) = \begin{bmatrix} 0 \\ 0 \\ 0 \end{bmatrix} R^n_b(0) = I$$

and consequently

$$p^b_{tb}(0) = \begin{bmatrix} 500 \\ 500 \\ 0 \end{bmatrix}, v^b_{nb}(0) = \begin{bmatrix} 0 \\ 0 \\ 0 \end{bmatrix}$$

The ARS bias is $b^b_{ars} = [0.012, -0.021, 0.014]^\top$, and the noise standard deviations are

$$\sigma_{acc} = 0.01 \frac{m}{s^2} \qquad \sigma_{ars} = 0.01 \frac{rad}{s} \qquad \sigma_{mag} = 0.01$$
$$\sigma_y = 1m \qquad \sigma_\partial = 0.01m$$

Lastly, the NLAO tuning parametres were chosen as $K_p = 10$, $k_I = 0.01$, and $\sigma = 1$. In the first minute of simulations, k_I were set to 0.1 to speed up convergence.

The scenario was simulated with two different initial estimates: One with small initial errors in order to view the steady state behaviour of the three-stage filters and one with large initial errors to view the transient behaviour. The estimates in the former case are initialized perfectly except for the ARS bias which is $\bar{b}^b_{ars}(0) = \hat{b}^{\bar{b}}_{ars}(0) = [0, 0, 0]^\top$. In the latter case, the initial estimates are

$$\bar{p}^b_{nb}(0) = \hat{p}^{\bar{b}}_{nb}(0) = \begin{bmatrix} 30 & 20 & 40 \end{bmatrix}$$
$$\bar{v}^b_{nb}(0) = \hat{v}^{\bar{b}}_{nb}(0) = \begin{bmatrix} 1 & -1 & 0.5 \end{bmatrix}$$
$$\begin{bmatrix} \phi & \theta & \psi \end{bmatrix} = \begin{bmatrix} 45^\circ & 45^\circ & 80^\circ \end{bmatrix}$$

where ϕ, θ, and ψ are the roll, pitch, and yaw angles, respectively. The initial ARS bias estimate is once again zero. The initial body-fixed estimates are found from the initial NED estimates. The initial covariance matrix for all filters in both simulation scenarios is $P(0) = \mathrm{diag}(l_3^\top, 10^{-3} l_3^\top)$.

The simulations last 600 seconds, the first 200 of which the vehicle stands still in order to let the estimators converge. The rate with which IMU measurements are retrieved, and consequently the update rate of the estimators, is 100 Hz. The iSBL measurements were gathered with 1 Hz.

The results of the simulations can be seen in Figure 3–6. Note that the estimates originally described in the body-fixed

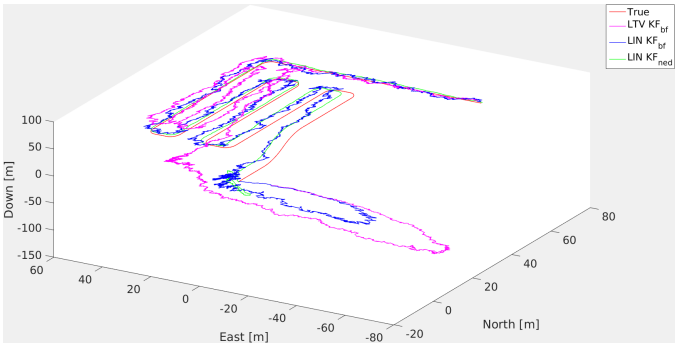

Fig. 3. True and estimated trajectories of the vehicle with small initial errors.

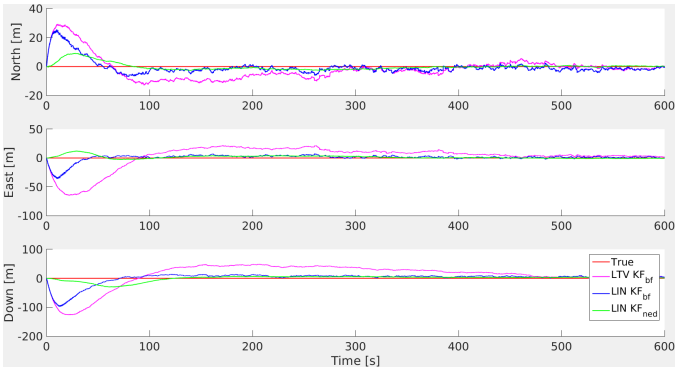

Fig. 4. The north, east, and down position estimate errors with small initial errors.

frame have been rotated by the true attitude to NED. The true attitude was used such that the position estimates could be compared without adding the effect of attitude estimate noise to either position estimate.

VI. Discussion

In Figure 3, the trajectory of the vehicle can be seen along with the LTV KF estimate and the linearized KF implemented with the body-fixed (subscript bf) and NED (subscript ned) formulation. From Figure 3–4, it is seen that the body-fixed filters are less accurate during the transient phase of the ARS bias estimate, seen in Figure 5 to last about 60 seconds. This is not surprising as it is part of

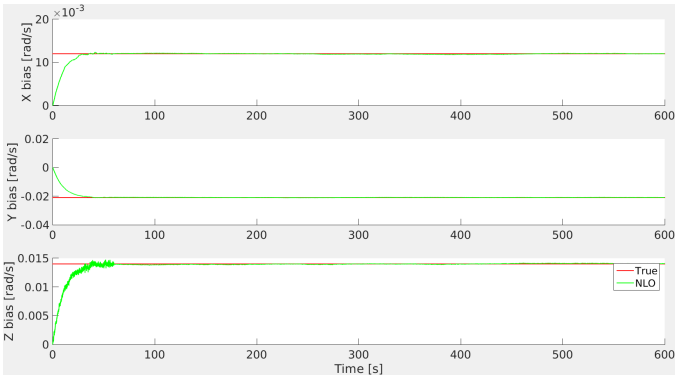

Fig. 5. The ARS bias estimate in the simulation with small initial errors.

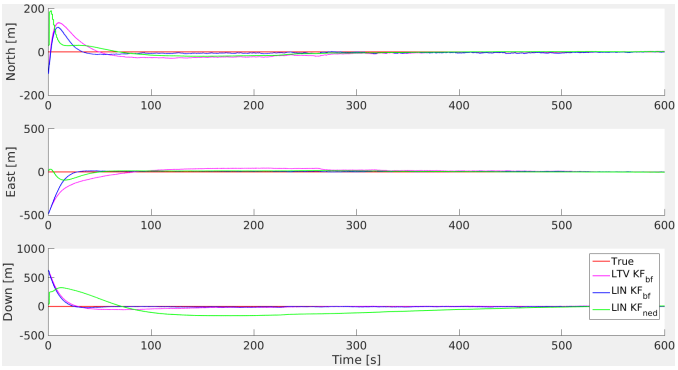

Fig. 6. The north, east, and down position estimate errors with large initial errors.

the body-fixed dynamics (10). The NED position estimate seems not to suffer much from this, as it both converges faster and deviates less than the body-fixed estimates. This is confirmed in Figure 4, where it can clearly be seen that the NED formulated linearized KF outperforms the body-fixed counterpart in steady-state.

In Figure 6, the position estimation errors in the case with large initial estimation errors is shown. Here, it can be seen that the body-fixed position estimates converge faster than the NED position estimate. This may explained by the observation

$$H_{xp,j}(\bar{x}) \approx \frac{(p^b_{bc_j} - p^b_{bc_m})^\top}{\|\check{\bar{p}}^b_{tb} + p^b_{bc_j}\|_2}$$

$$H_{\chi p,j}(\bar{\chi}, \check{z}) \approx \frac{\left(R^n_{\check{b}}(p^b_{bc_j} - p^b_{bc_m})\right)^\top}{\|\bar{p}^n_{nb} + R^n_{\check{b}} p^b_{bc_j} - p^n_{nt}\|_2}$$

From the above, we see that an error in the attitude estimate affects the NED formulated linearized KF more that the body-fixed one. In practice, it might make sense to let the NLAO converge for some time before turning on the translational motion estimators. This would be beneficial to both the body-fixed filters when there are small initial errors and the NED filter when there are large initial errors. Note that the difference in initial position estimate in Figure 6 is due to the large initial error in the attitude estimate. Since the true attitude was used to convert the body-fixed position estimate to NED position instead of the attitude estimate, the initial estimate appears more erroneous than it truly is.

In most applications of path planning, guidance, and control of the vehicle, the NED estimate will be preferred, and it will be better to use the linearized KF with the NED formulation. In addition to the NED esimate showing better performance in steady state, one would also get the benefit of not having to rotate the position estimate with a noisy attitude estimate.

VII. Conclusion

Two different three-stage filter solutions have been developed for the integration of IMU and iSBL measurements.

Two different three-stage filter solutions have been developed for the integration of IMU and iSBL measurements. The difference between the two solutions was the frame in which the last stage KF was formulated: in the body-fixed or the NED frame. Both solutions were implemented, simulated and compared. In the simulation study that was conducted, the three-stage filter with NED formulation in the last stage seemed to give better performance w.r.t. variance of the position estimate in steady-state, while showing slower convergence in the presence of large initial estimation errors. The latter could likely be improved by letting the NLAO converge for some time before turning on the translational motion estimator.

ACKNOWLEDGMENT

This work was funded by the Norwegian Research Council, Statoil, and FMC Technologies through the project Next Generation Subsea Inspection Maintenance and Repair (grant no. 234108). The project is associated with the Center of Autonomous Marine Operations and Systems (AMOS), grant no. 223254.

REFERENCES

[1] P. Batista, C. Silvestre, and P. Oliveira, "Single beacon navigation: Observability analysis and filter design," *American Control Conference (ACC), 2010*, pp. 6191–6196, 2010.

[2] ——, "GES integrated LBL/USBL navigation system for underwater vehicles," *Proceedings of the IEEE Conference on Decision and Control*, pp. 6609–6614, 2012.

[3] T. A. Johansen and T. I. Fossen, "The eXogenous Kalman Filter (XKF)," *International Journal of Control*, 2016.

[4] ——, "Nonlinear Observer for Tightly Coupled Integration of Pseudorange and Inertial Measurements," *IEEE Transactions on Control Systems Technology*, 2016.

[5] T. A. Johansen, T. I. Fossen, and G. C. Goodwin, "Three-stage filter for position estimation using pseudo-range measurements," *IEEE Transactions on Aerospace and Electronic Systems*, 2016.

[6] B. B. Stovner, T. A. Johansen, T. I. Fossen, and I. Schjølberg, "Three-stage Filter for Position and Velocity Estimation from Long Baseline Measurements with Unknown Wave Speed," in *Proc. of the American Contr. Conf.*, 2016, pp. 4532–4538.

[7] M. Morgado, P. Batista, P. Oliveira, and C. Silvestre, "Position and Velocity USBL / IMU Sensor-based Navigation Filter," *18th IFAC World Congress*, pp. 13 642–13 647, 2011.

[8] H. F. Grip, T. I. Fossen, T. A. Johansen, and A. Saberi, "Globally exponentially stable attitude and gyro bias estimation with application to GNSS/INS integration," *Automatica*, vol. 51, no. June, pp. 158–166, 2015.

[9] E. K. Jørgensen, T. A. Johansen, and I. Schjølberg, "Enhanced Hydroacoustic Range Robustness of Three-Stage Position Filter based on Long Baseline Measurements with Unknown Wave Speed," in *Conference on Control Applications in Marine Systems*, 2016.

[10] C. D. MEYER, "Generalized Inverses and Ranks of Block Matrices," *SIAM Review*, vol. 25, no. 4, pp. 597–602, 1973.

[11] R. E. Kalman and R. S. Bucy, "New results in linear filtering and prediction theory," *Journal of Basic Engineering*, vol. 83, no. 1, pp. 95–108, 1961.

[12] C.-T. Chen, *Linear System Theory and Design*, 3rd ed. Oxford University Press, Inc., 1998.